Modelling of $ZnS_xSe_{1-x}/ZnS_ySe_{1-y}$ band offsets and QW for green–yellow applications

2006 J. Phys.: Condens. Matter 18 3005

(http://iopscience.iop.org/0953-8984/18/11/007)

INSTITUTE OF PHYSICS PUBLISHING JOURNAL OF PHYSICS: CONDENSED MATTER

J. Phys.: Condens. Matter **18** (2006) 3005–3016 doi:10.1088/0953-8984/18/11/007

Modelling of $ZnS_xSe_{1-x}/ZnS_ySe_{1-y}$ band offsets and QW for green–yellow applications

S Abdi-Ben Nasrallah[1,3], N Sfina[1], N Bouarissa[2] and M Said[1]

[1] Département de Physique, Unité de Recherche de Physique des Solides, Faculté des Sciences de Monastir, 5019 Monastir, Tunisia
[2] Department of Physics, Faculty of Science, King Khalid University, Abha, PO Box 9004, Saudi Arabia

E-mail: samiaabdi@myway.com

Received 22 December 2005
Published 27 February 2006
Online at stacks.iop.org/JPhysCM/18/3005

Abstract

II–VI quantum well (QW) structures are now the subject of an increasing number of studies due to their applications in optoelectronics. Following our recent calculations showing that the fundamental gap of ZnS_xSe_{1-x} presents a minimum for sulfur molar fraction $x = 0.20$, an accurate knowledge of band offsets for these ternary alloys will be useful to model devices based on $ZnS_xSe_{1-x}/ZnS_ySe_{1-y}$ QWs. With this aim, we have calculated the electronic band parameters for this system. Hence, and using the model-solid theory, strain effects of electrons, heavy holes (hh) and light holes (lh) are investigated as a function of sulfur composition in the hole range $0 \leqslant x, y \leqslant 1$. Taking into account these results and based on a one-dimensional Schrödinger equation, we report a calculation of level energies in $ZnS_xSe_{1-x}/ZnS_{0.8}Se_{0.2}$ QWs for $0 \leqslant x \leqslant 0.2$, which depend on the thickness of the layers as well as on the composition of the ternary alloys. Our result provides useful information for experimentalists and opens the way to realize optoelectronic devices intended to operate in the whole range of the visible spectrum and based on $ZnS_xSe_{1-x}/ZnS_ySe_{1-y}$.

(Some figures in this article are in colour only in the electronic version)

1. Introduction

The II–VI semiconductors (SCs) could form the basis for a variety of efficient light-emitting devices spanning the entire range of the visible spectrum since their bandgaps range from the infrared to the ultraviolet [1]. Despite the fact that the direct-bandgap II–VI SCs are the most promising for realizing visible laser diodes (LDs) [2] and efficient light-emitting-diode (LED) [3] displays, major difficulties soon emerged with these materials. This can be

[3] Author to whom any correspondence should be addressed.

generally defined in terms of structural and electronic quality of the material [1, 4]. In contrast, research on III–V compounds has progressed quite rapidly. This progress was possible with development of growth techniques which were also applied with success to the studies of II–VI compounds [5, 6]. The evolution in growth techniques prompted studies and extensive research effort has been invested in recent years in the study principally of II–VI and III–V nitride wide-gap SCs as well as their ternary [7] and quaternary [8] alloys covering a wide spectral range from visible to ultraviolet. However, the II–VI heterostructures remain the most natural candidates for blue–green laser diode applications [9] not only because this spectral range (>450 nm) is hardly reachable by III–V nitride based lasers [10] but also due to the gradual interface effects on the confinement properties of III–V nitride QWs such as GaN/AlGaN. This makes important other wide-gap SCs like ZnSSe/ZnSe [11] with its strong abrupt interface. In fact, zinc selenide (ZnSe) is the starting material for a large number of II–VI SC ternary and quaternary alloys which can be incorporated into multilayer structures and devices such as lasers and light emitting diodes (LEDs) [12, 13] and the primary recent need is in the area of optical storage [1]. Because of the small mismatch of ZnSe with GaAs, most of the ZnSe LED and LD devices are fabricated on GaAs substrates [1, 14]. However, the quality of ZnSe-based heterostructures grown on GaAs substrates is limited by other structural defects due to the lattice relaxation. To avoid these unwanted defects, we have focused on modelling LEDs and LD structures using ZnS_xSe_{1-x} material on a ZnS_ySe_{1-y} substrate, which eliminates many of the problems associated with lattice mismatch and surface defects. In fact, with ZnS_xSe_{1-x}/ZnSe heterostructures, emission wavelength can be tuned gradually from the blue (ZnSe) to the UV (ZnS) [15] range with increasing x in the alloy, but the corresponding decrease in lattice parameter also increases the lattice mismatch with the substrate and large strains are present in the pseudomorphic QWs. The use of the ZnS_ySe_{1-y} substrate is a potential advantage of ZnS_xSe_{1-x} material with $0 \leqslant x, y \leqslant 1$, and then the strain effect is reduced.

Until recently, it was commonly accepted that the bandgap of ZnSSe increases more or less monotonically with increasing sulfur content from $E_g(\mathrm{ZnSe}) = 2.80$ eV to $E_g(\mathrm{ZnS}) = 3.67$ eV [16]. But taking into account the recent behaviour of the ZnS_xSe_{1-x} gap, we can obtain ternary materials spanning bandgaps within the range 2.60–3.67 eV [17]. In fact, we have shown that the sulfur incorporation generates significant effects on the bandgap variation: the bandgap decreases with increasing sulfur content until 2.60 eV for $x = 0.2$, and then increases up to 3.67 eV for ZnS. Such a strong deviation from the typically expected behaviour is very important for device applications and has prompted us to perform band offset calculations.

Therefore, and using the model solid theory (MST) [18], the valence and conduction band offsets (BOs) for $ZnS_xSe_{1-x}/ZnS_ySe_{1-y}$ heterostructures ($0 \leqslant x, y \leqslant 1$) are calculated. Using these band offsets, we have simulated $ZnS_xSe_{1-x}/ZnS_{0.8}Se_{0.2}$ and obtained results which can be useful for experimental investigations. The thickness and composition ($0 \leqslant x \leqslant 0.20$) of this single QW are computed to get the optimum confinement of the interband electron–hole transition and the optimum out of plane oscillator strength and wavefunction overlap.

In this work, we report in section 2 calculations of electron, heavy hole and light hole band offsets. These parameters with the effective masses are used to simulate and optimize the interband electron–hole transition. Results of well thickness and sulfur composition variations are summarized in section 3.

2. Calculation of band offsets

With the improvement of growth techniques (in particular, molecular beam epitaxy, MBE), it has become possible to grow SC superlattices and tailor the band structures to achieve

the desired properties and device applications. The lattice mismatch between SCs can be accommodated by lattice strains in sufficiently thin layers which can cause profound changes in the electronic properties and therefore provides extra flexibility in device design. The knowledge of the discontinuities in valence and conduction bands at SC interfaces is essential for the analysis of the properties of any heterojunction. In fact, in the case of ZnSSe based heterostructures, the recently reported variation gap with sulfur composition emphasizes the need to research relevant fundamental valence and conduction band offsets (BOs) of heterostructures. To evaluate these band offsets, the model-solid theory of Van Der Walle and Martin [18] is practical and can be used for lattice-matched and lattice-mismatched interfaces. The authors consider an energy reference level for valence band $E_{v,av}$ defined as the average over the uppermost valence bands at the Γ point of the Brillouin zone.

In this section, we present calculations of BOs for the $ZnS_xSe_{1-x}/ZnS_ySe_{1-y}$ interface with $0 \leqslant x, y \leqslant 1$. The lattice parameter for ZnSe is 0.566 86 nm and the one of ZnS is 0.540 93 nm. For the ternary alloy, the lattice parameter is estimated from the Vegard's law. Therefore, when growing the ZnS_xSe_{1-x} layer on the ZnS_ySe_{1-y} substrate in the z-axis direction of growth, a deformation of the crystal lattice takes place. We consider that the strain direction is the one for which z axis is oriented along the [001] crystallographic direction. Pseudomorphic growth of an overlayer on a substrate with different lattice constants introduces strain components. Under pseudomorphic conditions, strains are sufficiently small to be in the linear regime. Our procedure has been to use calculated valence-band positions and add the reported bandgap to obtain conduction-band positions.

The ZnSe and ZnS semiconductors have the zinc-blende structure with a band structure that includes three valence bands at Γ. In the absence of strain and spin–orbit splitting, these bands are degenerate. The spin–orbit interaction splits them into heavy and light hole bands (hh and lh) and the spin–orbit band (so). The hydrostatic strain shifts the average valence band energy and the conduction band while the shear component of strain splits the degeneracy of the light and the heavy hole valence bands when coupled to the spin–orbit interaction.

The band energy shifts are related to strains by making use of deformation potentials. For strain along the [001] direction of the $ZnS_xSe_{1-x}/ZnS_ySe_{1-y}$ heterostructure, the shifts of the valence bands are given by [18]

$$\delta E_{v,hh} = a_v(2\varepsilon_\parallel + \varepsilon_\perp) - 0.5\delta E_{001}$$
$$\delta E_{v,hh} = 2a_v\varepsilon_\parallel\left(1 - \frac{C_{12}}{C_{11}}\right) - 0.5\delta E_{001} \tag{1}$$

$$\delta E_{v,lh} = 2a_v\varepsilon_\parallel\left(1 - \frac{C_{12}}{C_{11}}\right) - \frac{\Delta_0}{2} + 0.25\delta E_{001} + 0.5[\Delta_0^2 + \Delta_0\delta E_{001} + 2.25(\delta E_{001})^2]^{1/2} \tag{2}$$

$$\delta E_{v,so} = 2a_v\varepsilon_\parallel\left(1 - \frac{C_{12}}{C_{11}}\right) + \frac{\Delta_0}{2} + 0.25\delta E_{001} - 0.5[\Delta_0^2 + \Delta_0\delta E_{001} + 2.25(\delta E_{001})^2]^{1/2}. \tag{3}$$

In these equations, δE_{001} is given by

$$\delta E_{001} = 2b(\varepsilon_\perp - \varepsilon_\parallel)$$
$$\delta E_{001} = -2b\varepsilon_\parallel\left(2\frac{C_{12}}{C_{11}} + 1\right). \tag{4}$$

The components of the strain tensor for ZnS_xSe_{1-x}, $\varepsilon_{xx} = \varepsilon_{yy} = \varepsilon_\parallel$ and $\varepsilon_{zz} = \varepsilon_\perp$ are given by

$$\varepsilon_\parallel = \frac{a_\parallel}{a} - 1 \tag{5}$$

$$\varepsilon_\perp = -2\frac{C_{12}}{C_{11}}\varepsilon_\parallel \tag{6}$$

with $a_{\parallel}$ and a are the substrate and the unstrained over-layer lattice constants while $a_{\perp}$ is the perpendicular over-layer lattice constant given, in the [001] direction, by

$$a_{\perp} = a\left\{1 - 2\frac{C_{12}}{C_{11}}\left(\frac{a_{\parallel}}{a} - 1\right)\right\}. \tag{7}$$

Δ_0 is the spin–orbit splitting, a_v and b are the hydrostatic and the shear deformation potential for the valence band and C_{ij} specify the bulk elastic coefficients for the material under consideration.

The first terms in the valence band shifts are the hydrostatic corrections and the second are the shear ones. Equations (1)–(3) show that the heavy holes remain uncoupled to the light holes, while the light holes and the split-off bands are coupled by the strain and the spin orbit splitting. We notice that the hydrostatic component of the strain is the same for hh, lh and so.

Seeing that the ZnSSe alloy has a direct gap all along the sulfur composition range, the shear strain has no effect on the energetic position of the conduction band and there is only a hydrostatic CB correction due to the strain. This component is given by

$$\begin{aligned} \delta E_c &= a_c(2\varepsilon_{\parallel} + \varepsilon_{\perp}) \\ \delta E_c &= 2a_c\varepsilon_{\parallel}\left(1 - \frac{C_{12}}{C_{11}}\right) \end{aligned} \tag{8}$$

a_c being the hydrostatic deformation potential for the conduction band.

Consequently, the valence and conduction band offsets including strain effects for the $ZnS_xSe_{1-x}/ZnS_ySe_{1-y}$ heterojunction are

$$\begin{aligned} \Delta E_v &= [E_v^{uns}(ZnS_xSe_{1-x}) + \delta E_v^{hyd} + \delta E_v^{sh}] - E_v^{uns}(ZnS_ySe_{1-y}) \\ \Delta E_v &= \Delta E_v^{uns} + \delta E_v^{hyd} + \delta E_v^{sh} \\ \Delta E_{v,hh,lh,so} &= \Delta E_v^{unst} + \delta E_{v,hh,lh,so} \end{aligned} \tag{9}$$

$$\Delta E_c = \Delta E_v^{unst} + \Delta E_g^{unst} + \delta E_c \tag{10}$$

where δE_v^{hyd} is the hydrostatic component of the strain while δE_v^{sh} is the shear component; ΔE_g^{unst} represents the bandgap difference between ZnS_xSe_{1-x} and ZnS_ySe_{1-y} unstrained bulk materials. Note that equations (9) and (10) result from an approximation since the band offset modification due to the strain-induced charge transfers at the interface is neglected. The bandgap energy for the alloy ZnSSe is taken from our calculations in [17] and given by the expression

$$E_g^{\Gamma}(x) = 2.80 - 2.26x + 7.55x^2 - 4.43x^3 \tag{11}$$

showing an equivalent bowing parameter b that is $b(x) = -4.43x + 3.13$.

Note that b is strongly composition dependent, leading to a non-linear and non-monotonic composition dependence of the bandgap. It is worth mentioning that in the present study we have used the same room temperature bandgaps of ZnSe and ZnS as were used in our previously published work [17], i.e. 2.80 and 3.67 eV, respectively.

Using the above equations, we have calculated the band offsets for strained $ZnS_xSe_{1-x}/ZnS_ySe_{1-y}$ for the range $0 \leqslant x, y \leqslant 1$. The parameters related to the strain adopted in this work [19] are listed in table 1. The data for ZnS_xSe_{1-x} alloys are evaluated from a linear interpolation of the parameters listed in table 1. Results are depicted as a function of x and y compositions in figures 1(a) and (b) for electrons. For heavy and light holes, the iso-energy band offsets are practically linear. The laws

$$\begin{aligned} \Delta E_{v,hh}(x, y) &= (y - x)[0.95 - 0.05x + 0.001x(x + y) - 0.01y] \\ \Delta E_{v,lh}(x, y) &= (y - x)[0.788 - 0.14x + 0.01\sqrt{x}(x + y) - 0.01y] \end{aligned}$$

Table 1. Spin–orbit splitting Δ_0, the average energy of the three uppermost valence bands $E_{v,av}$, experimental values of hydrostatic deformation potential for the valence and conduction bands a_v and a_c, experimental uniaxial deformation potential b. All these parameters are in eV. The elastic constants C_{11} and C_{12} are in 10^{10} N m^{-2} [21].

	Δ_0	$E_{v,av}$	a_v	a_c	b	C_{11}	C_{12}
ZnSe	0.43	−8.37	1.65	4.17	−1.2	8.95	5.39
ZnS	0.07	−9.15	2.3	−4.09	−0.80	9.81	6.27

give good approximate analytical expressions for the heavy and light hole valence band discontinuities. Note that all band offsets are given in electron volts (eV). According to our band offset calculations, we found the following results.

(i) The band offsets are large in the valence band (from −0.90 to 0.90 eV for $0 \leqslant x, y \leqslant 1$), but small in the conduction band (from −0.45 to 0.45 eV for $0 \leqslant x, y \leqslant 1$). This is expected in this mixed anion system. Wei *et al* [20] attributed the large VBO to the fact that the VBO is an anion p-like state and the anion p-orbital energies increase significantly with the anion atomic number while the CBO is mostly a cation s state with only minor contributions from anion s orbitals.

(ii) The valence band offsets increase (decrease) when ZnS_xSe_{1-x} is under compressive (tensile) strain. Note that under compressive strain (growth on a substrate with smaller lattice constant $x < y$) the heavy hole band will be at the band edge ($\delta E_{v,hh} > \delta E_{v,lh}$).

(iii) The plots show drastic changes relative to those commonly accepted for conduction band offset. In the case of $ZnS_xSe_{1-x}/ZnS_ySe_{1-y}$, $0 \leqslant x \leqslant 1$ and $y = 0.8$, the valence band discontinuity for heavy holes $\Delta E_{v,hh}$ spans the range −0.18 to 0.76 eV while the conduction band discontinuity ΔE_c decreases from −0.25 to −0.33 eV, then increases to 0.045 eV, and after that it decreases until −0.42 eV (figure 2(a)). Using these values, the strained band line-up of the $ZnS_xSe_{1-x}/ZnS_{0.8}Se_{0.2}$ quantum well (QW) with $0 \leqslant x \leqslant 0.20$ is of type I ($0.57 \leqslant \Delta E_{v,hh} \leqslant 0.76$ eV and $-0.33 \leqslant \Delta E_c \leqslant -0.25$ eV) while the optical transition in the $ZnS_xSe_{1-x}/ZnSe$ structure becomes of type II for sulfur molar fraction lower than 32% and higher than 95% (figure 2(b)). For $ZnS_xSe_{1-x}/ZnS_{0.8}Se_{0.2}$ heterostructure with $0 \leqslant x \leqslant 0.2$, the material undergoes compressive strains in the growth direction due to the neighbouring $ZnS_{0.8}Se_{0.2}$ which has a smaller lattice constant; therefore the bandgap of ZnS_xSe_{1-x} at the lateral interface becomes small.

(iv) Despite the promising technological applications of ZnSSe material/ZnSSe substrate QWs, we could not find any experimental work in the literature. However, Maia *et al* [21] have studied the band offsets of $ZnSe/ZnS_{0.18}Se_{0.82}$ strained QWs and reported values of 192 and 135 meV for $\Delta E_{v,hh}$ and $\Delta E_{v,lh}$, respectively. Our calculated values of $\Delta E_{v,hh}$ and $\Delta E_{v,lh}$ are found to be 172 and 130 meV, respectively, which are in good agreement with those of [21]. The small discrepancy in our CBO values and those given in [21] is probably due to the atypical behaviour of the ZnSSe bandgap used in our calculation. New experimental and theoretical results for other sulfur compositions would be useful for a detailed comparison with our calculations.

3. Electronic properties of $ZnS_xSe_{1-x}/ZnS_{0.8}Se_{0.2}$ single quantum well

The heterostructure for modelling consists of two $ZnS_{0.8}Se_{0.2}$ barriers separated by a ZnS_xSe_{1-x} ($0 \leqslant x \leqslant 1$) QW of thickness L_w. A $ZnS_xSe_{1-x}/ZnS_ySe_{1-y}$ single QW is used since the transitions are much sharper than in a multiple-QW structure or superlattice.

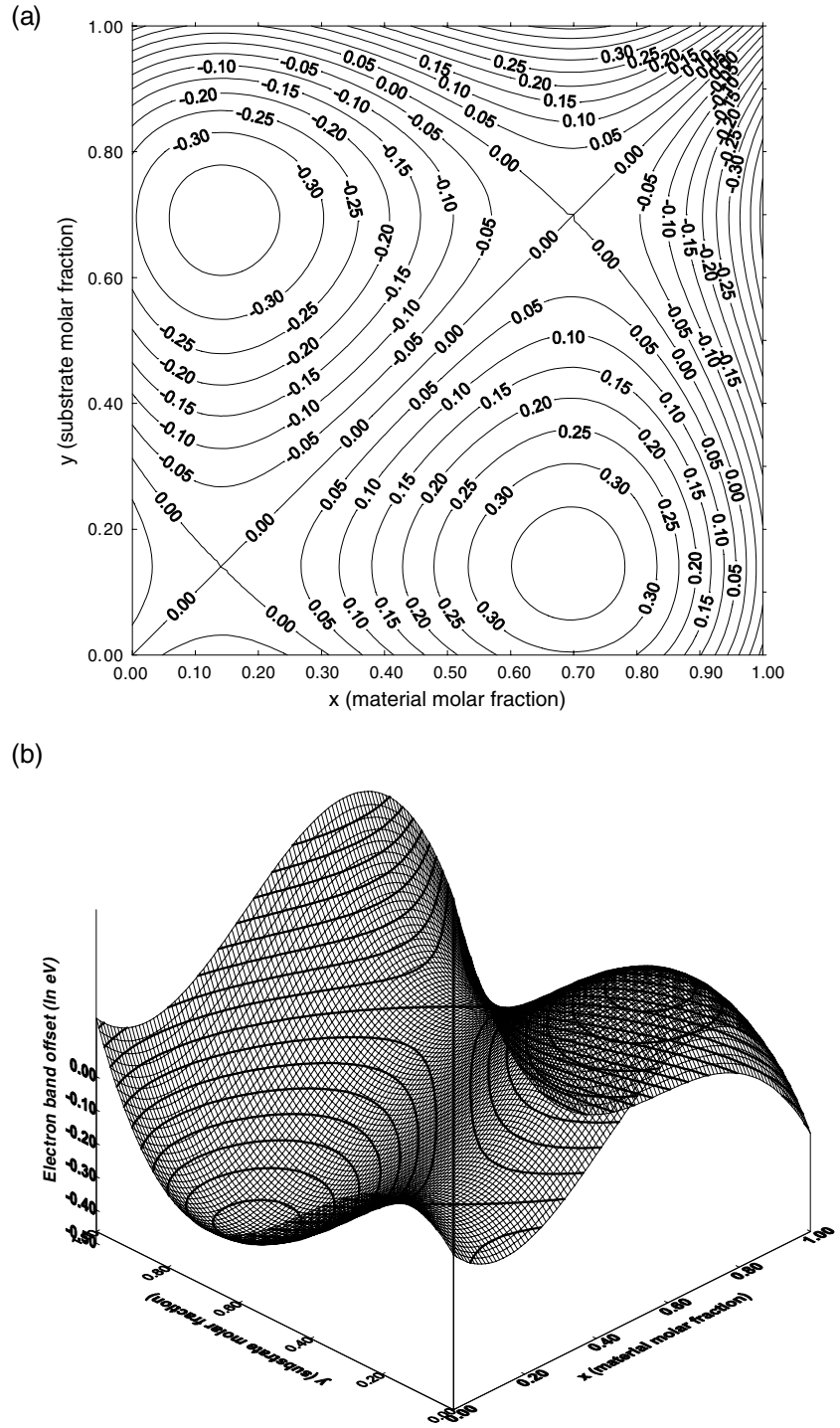

Figure 1. (a) Conduction band offset ΔE_c in (001) $ZnS_xSe_{1-x}/ZnS_ySe_{1-y}$ interface. (b) A three-dimensional representation of ΔE_c. All band offsets are given in eV.

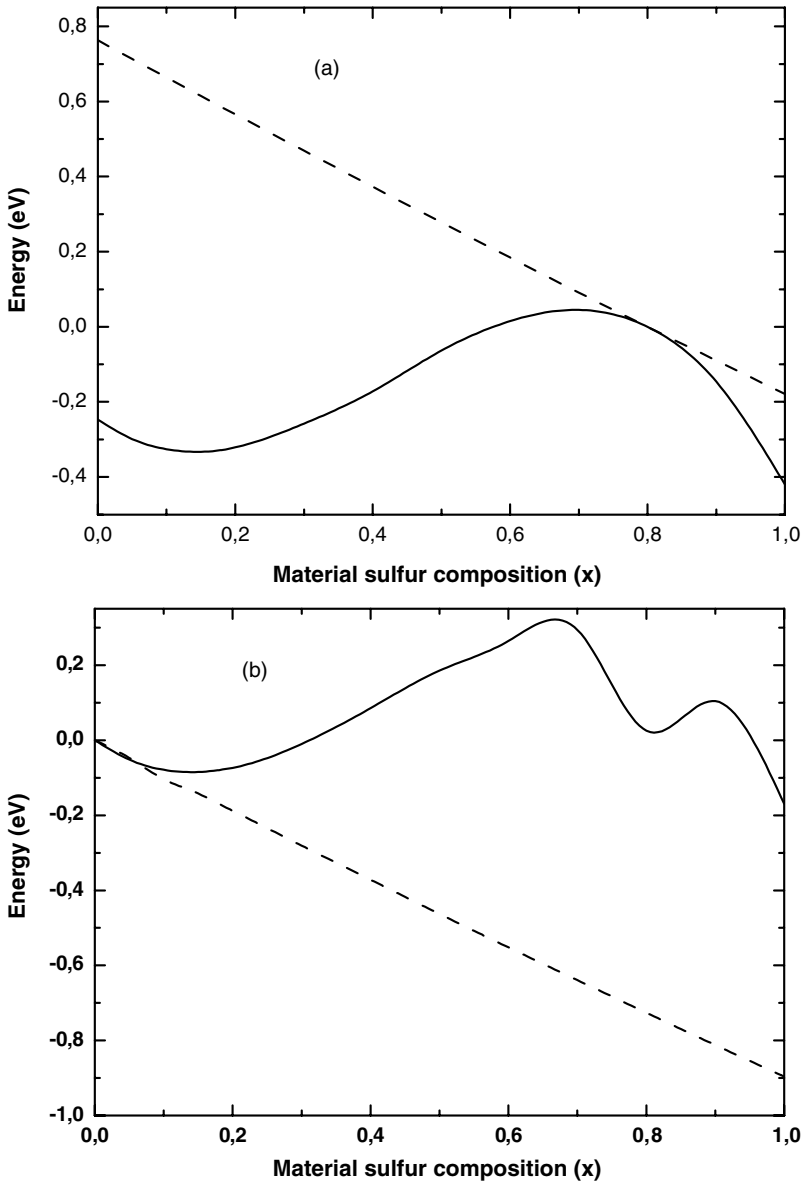

Figure 2. The valence (dashed line) and the conduction (solid line) band discontinuities at the (a) $ZnS_xSe_{1-x}/ZnS_{0.8}Se_{0.2}$ and (b) $ZnS_xSe_{1-x}/ZnSe$ interfaces.

Based on an empirical pseudopotential method [22], and for a parabolic fit of the conduction band dispersions for ZnS_xSe_{1-x} alloy, we have calculated the electron effective mass m^* at the minimum of the CB [17].

The fitted expression

$$m_e^*(x) = 0.193 - 0.064x + 0.160x^2 \tag{12}$$

gives m^* for any sulfur molar fraction. Due to the lack in the hole effective masses of ZnSSe alloys, for the heavy and light holes in ternary compounds we opt for linear interpolation

Table 2. Values of effective masses for electrons and heavy and light holes denoted respectively m_e^*, m_{hh}^* and m_{lh}^* evaluated in units of the free electron mass m_0.

	$x = 0$	$x = 0.1$	$x = 0.2$	$x = 0.8$	$x = 1$
m_e^*	0.19	0.19	0.19	0.24	0.27
m_{hh}^*	1.2	1.3	1.4	1.8	1.76
m_{lh}^*	0.15	0.15	0.155	0.19	0.23

Table 3. Calculated conduction (ΔE_c) and valence ($\Delta E_{v,hh}$, $\Delta E_{v,lh}$) band offsets for strained ZnS_xSe_{1-x} with $x = 0$, 0.1 and 0.2 on relaxed $ZnS_{0.8}Se_{0.2}$ substrate given in eV.

	$x = 0$	$x = 0.1$	$x = 0.2$
ΔE_c	−0.25	−0.33	−0.32
$\Delta E_{v,hh}$	0.76	0.66	0.57
$\Delta E_{v,lh}$	0.62	0.54	0.46

between masses of the two binary parents. The results of calculation are summarized in table 2. The conduction and valence band discontinuities for the $ZnS_xSe_{1-x}/ZnS_{0.8}Se_{0.2}$ QW under investigation ($x = 0$, 0.1, 0.2 and $y = 0.8$) calculated in section 2 are listed in table 3.

To evaluate electronic states of the heterostructure under investigation, we have used the model described in our paper [23]. We started by solving the one-dimensional Schrödinger equation in the growth direction using the effective mass theory [24]. In the single-band version of the envelope function approximation, the eigenvalues E_ν and eigenfunctions Φ_ν for subbands ν are determined by solving the one-dimensional Schrödinger equation:

$$\left[\frac{-\hbar^2}{2}\frac{\mathrm{d}}{\mathrm{d}z}\frac{1}{m^*(z)}\frac{\mathrm{d}}{\mathrm{d}z} + V_B(z) - E_\nu\right]\phi_\nu(z) = 0 \tag{13}$$

where z is the growth direction, $\hbar$ is the Planck's constant, $m^*(z)$ is the electron (heavy hole) effective mass, ν is the subband index and $V_B(z)$ is the potential energy due to the heterostructure conduction (valence) band-edge discontinuities calculated in section 2. Numerically, the problem was treated using the finite differential method.

First, we have plotted the bandgap energies for relaxed ZnSSe and strained ZnSSe on $ZnS_{0.8}Se_{0.2}$ substrate in the whole range of sulfur molar fraction x (figure 3). As can be seen, the strain causes a redshift in the bandgap.

Furthermore, we have illustrated the subband energies for $x = 0$ (solid line), 0.1 (dashed line) and 0.2 (dotted line) as a function of the well width L_w (figure 4 plot (a)). The plot shows that the energy levels increase until $L_w = 2$ nm for heavy holes and approximately $L_w = 4$ nm for electrons and light holes and then become stationary; the electron energy levels are nearly the same with $x = 0.1$ and 0.2. As can be seen, the subband energies increase with the well thickness L_w of the ZnS_xSe_{1-x} layer. Therefore, we have exhibited in figure 4 (plot (b)) the emission energies for the fundamental transitions e_1–hh_1 and e_1–lh_1 with $x = 0$ (solid line), $x = 0.1$ (dashed line) and $x = 0.2$ (dotted line). As shown, the emission energy of the e_1–hh_1 (e_1–lh_1) transition undergoes a redshift with increasing L_w but increases with sulfur composition x. The transition energy e_1–lh_1 has the same value for $x = 0$ and 0.1.

Since save for the blue and the red emissions there are no green–yellow commercialized LDs yet, we have focused our attention on this wavelength range (550–585) nm.

It is clear that by varying the well thickness it is possible to realize $ZnS_xSe_{1-x}/ZnS_{0.8}Se_{0.2}$-based devices that can be tuned to emit throughout the green, yellow and orange by changing only the QW layer thickness or the sulfur composition x. With the e_1–hh_1 transition, we

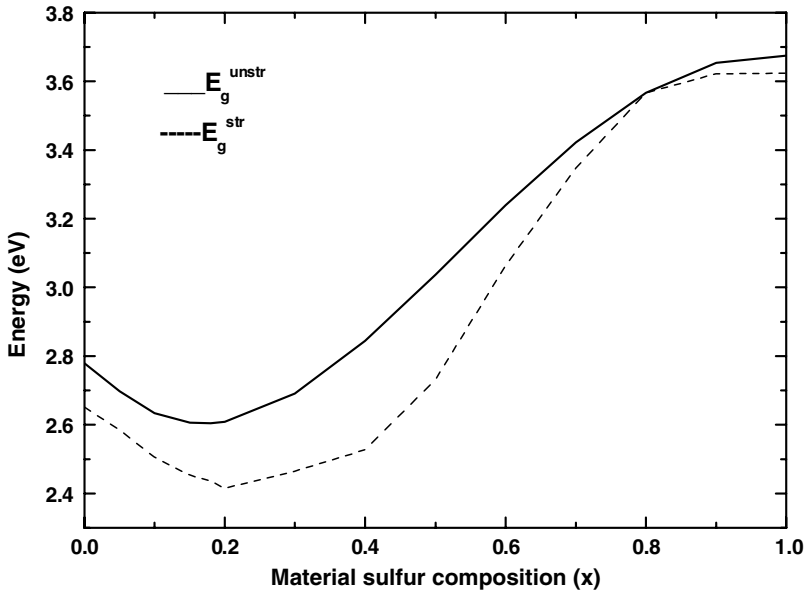

Figure 3. The relaxed bandgap of bulk material ZnS_xSe_{1-x} (solid line) and strained (dashed line) bandgaps of ZnS_xSe_{1-x} on $ZnS_{0.8}Se_{0.2}$ relaxed substrate as a function of sulfur molar fraction x.

can achieve for sulfur molar fraction $x = 0, 0.1, 0.2$ the green emission (2.15 eV) with $L_w \approx 0.7, 0.9, 1$ nm, the yellow (2.12 eV) with $L_w \approx 0.8, 0.9, 1.2$ nm and the orange (1.92 eV) with $L_w \approx 1.3, 1.5, 2$ nm, respectively. With the e_1–lh_1 transition, the same wavelengths are accomplished as follows: the green with $L_w \approx 1.7, 1.7, 2$ nm, the yellow with $L_w \approx 1.9, 1.9, 2.3$ nm and the orange with $L_w \approx 3.5, 3.5, >5$ nm, respectively. Therefore, we have chosen the compositions and well thicknesses accessible in a realistic way for epitaxial growth, $L_w = 1$ nm, $x = 0.2$; $L_w = 1.2$ nm, $x = 0.2$ and $L_w = 2$ nm, $x = 0.2$ respectively for green, yellow and orange. To study and carry out the quantum efficiency of our designs with these sets of parameters, we have calculated (i) the oscillator strength of the e–hh transition, which is defined by the expression [25]

$$f_{l\to k} = \frac{2m_0}{\hbar^2}(E_l - E_k)|\langle\phi_l|z|\phi_k\rangle|^2 \tag{14}$$

where m_0 is the free electron mass, $(E_l - E_k)$ is the energy difference between the initial and final states and $|\langle\phi_l|z|\phi_k\rangle|$ is the dipole matrix element of the transition, and (ii) the wavefunction overlap, defined as

$$|\langle\phi_l \mid \phi_k\rangle|^2. \tag{15}$$

The oscillator strength is of the order of 10^4 arbitrary units, which is better than the oscillator strength obtained with SiGe-based structures (from 10^2 to 10^3) [26, 27] and InGaN heterostructures (10^3) [28]. The wavefunction overlap of 65, 68 and 83% for the type I green, yellow and orange transitions respectively is also excellent while it is at least 49% in the $Si_{1-y}Ge_y/Si/Si_{1-x}Ge_x/Si/Si_{1-y}Ge_y$ structure with $x = 0.7$, $y = 0.25$ [26]. The edges of the conduction and valence bands of our simulated and optimized designs for the green, yellow and orange wavelengths are illustrated in figure 5. The fundamental electron and heavy hole levels with their relative wavefunctions are also shown.

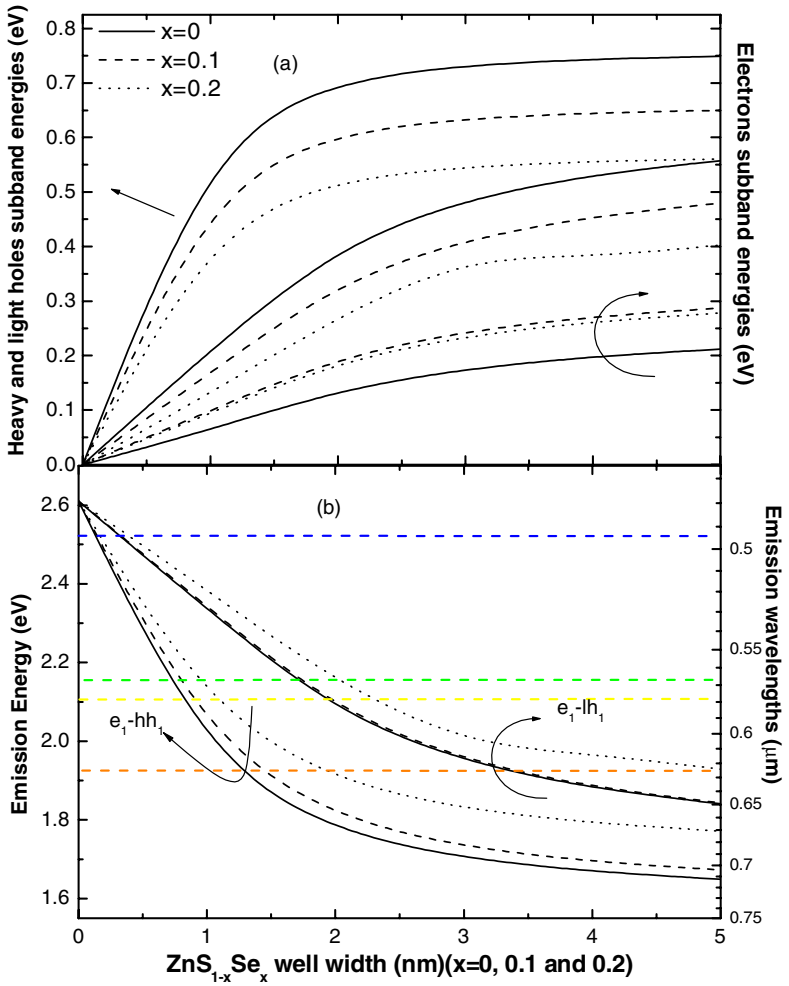

Figure 4. (a) Electron, heavy hole and light hole confinement energies for the $ZnS_xSe_{1-x}/ZnS_{0.8}Se_{0.2}$ structure as a function of the ZnS_xSe_{1-x} well width L_w with values of $x = 0$ (solid line), $x = 0.1$ (dashed line) and $x = 0.2$ (dotted line). (b) Deduced evolutions of the e_1–hh_1 and e_1–lh_1 transition energies versus the ZnS_xSe_{1-x} layer thickness. Energies are determined by the envelope function approximation and given in eV.

4. Conclusions

The progress in growth techniques makes it possible to create heterostructures which allow a great flexibility in design by varying the alloy concentrations, the thickness layers and the state of strain. Therefore, the knowledge of the band offsets is crucial to clarify confinement properties of electrons and holes, a necessary step to describe the role of confinement in the gain mechanism of laser devices. The ZnS_xSe_{1-x} bandgap that we have recently reported motivates us to perform band offset calculations of heterostructures. Thus, by means of the model-solid theory, we have estimated the valence and conduction band offsets for the pseudomorphically strained $ZnS_xSe_{1-x}/ZnS_ySe_{1-y}$ interface by using our recent bandgap calculation. As can be seen, the system can be from type I or type II for a material under compressive or tensile strain according to x and y concentrations.

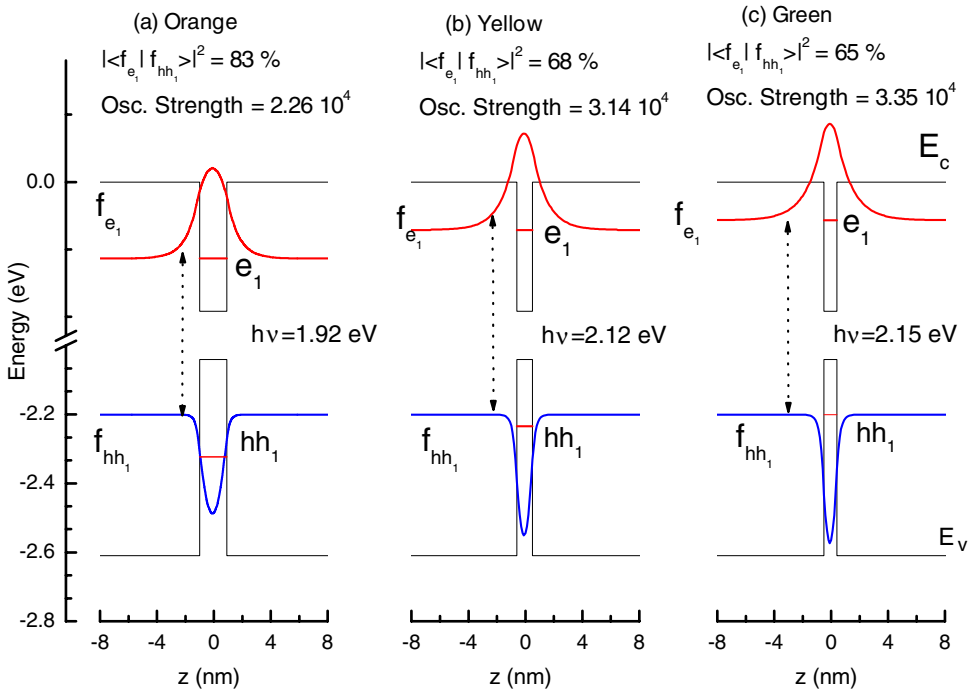

Figure 5. Conduction and valence band edge minima for $ZnS_xSe_{1-x}/ZnS_{0.8}Se_{0.2}$ structure versus the ZnS_xSe_{1-x} well width L_w. (a) Orange emission (1.92 eV) obtained with $L_w = 2$ nm and $x = 0.2$. (b) Yellow emission (2.12 eV) obtained with $L_w = 1.2$ nm and $x = 0.2$. (c) Green emission (2.15 eV) obtained with $L_w = 1$ nm and $x = 0.2$. The fundamental levels for electrons and heavy holes with their relative wavefunctions are illustrated. The oscillator strength of the fundamental transition e_1–hh_1 and wavefunction overlap are also depicted.

GaAs is commonly used for ZnSe-based optoelectronic structures, which, indeed, lead to some problems with twins and other defects. To circumvent these problems, we suggest the use of ZnSSe substrates. Such substrates may be available with the advent of growth technology. Our calculations permit us to avoid many problems related to lattice mismatch and surface defects hindering the development of ZnSe II–VI devices. We have simulated a ZnS_xSe_{1-x} single QW with $0 \leqslant x \leqslant 0.2$ on a ZnS_ySe_{1-y} substrate ($y = 0.8$) with the purpose of modelling ZnSSe based LDs emitting in the 500–600 nm range since there are no commercialized green, yellow and orange LDs yet. As described, ZnS_xSe_{1-x} can cover a considerable part of the colour diagram when growing on $ZnS_{0.8}Se_{0.2}$ substrate. The green, yellow or orange emission can be achieved with the e_1–hh_1 (or e_1–lh_1) transition energies by varying the thickness well and the alloy composition in a realistic way for epitaxial growth.

In conclusion, our BO calculations can be useful to provide a reference in the design of ZnSSe based device applications. The results presented have evidenced a large potential of the II–VI wide bandgap compounds SCs for practical application of the green, yellow and orange emissions.

References

[1] Gunshor R L and Nurmikko A V 1995 *MRS Bull.* **20** 15
[2] Klude M, Alexe G, Kruse C, Passow T, Heinke H and Hommel D 2002 *Phys. Status Solidi* b **229** 935

[3] Chang J H, Song J S, Godo K, Yao T, Shen M Y and Goto T 2001 *Appl. Phys. Lett.* **78** 566
[4] Cook J W Jr and Schetzina J F 1995 *Laser Focus World* **31** 101
[5] EHC 1985 *The Technology and Physics of Molecular Beam Epitaxy* (New York: Plenum)
[6] Gunshor R L, Kolodziejski L A, Nurmikko A V and Otsuka N 1990 *Semiconductors and Semimetals* vol 33, ed T Pearsall (New York: Academic)
[7] Muñoz M, Lu H, Zhou X and Tamargo M C 2003 *Appl. Phys. Lett.* **83** 1995
[8] Vurgaftman I, Meyer J R and Ram-Mohan L R 2001 *J. Appl. Phys.* **89** 5815
[9] Kato E, Noguchi H, Nagai M, Okuyama H, Kijima S and Ishibashi A 1998 *Electron. Lett.* **34** 282
[10] Nakamo K and Ishibashi A 1997 *Mater. Sci. Forum* **1329** 258
[11] Hermans J, Woitok J, Schiffers W, Geurts J, Schneider A, Scholl M, Sollner J and Heuken M 1994 *J. Cryst. Growth* **138** 612
[12] Okuyama H, Nakamo K, Miyajima T and Akimoto K 1992 *J. Cryst. Growth* **117** 139
[13] Reuscher G, Keim M, Lugauer H J, Waag A and Landwehr G 2000 *J. Cryst. Growth* **214/215** 1071
[14] Kolodziejski L A, Gunshor R L and Nurmikko A V 1995 *Annu. Rev. Mater. Sci.* **25** 711
[15] Mayer H and Rossler U 1993 *Solid State Commun.* **87** 81
[16] Palmer D W 2002 Properties of the semiconductors http://www.semiconductors.co.uk
[17] BenNasrallah S A, Ben Afia S, Belmabrouk H and Said M 2005 *Eur. Phys. J.* B **43** 3
[18] Van de Walle C G 1989 *Phys. Rev.* B **39** 1871
[19] Shahzad K, Olego D J and Van de Walle C G 1988 *Phys. Rev.* B **38** 1417
[20] Wei S H, Zhang S B and Zunger A 2000 *J. Appl. Phys.* **87** 1304
[21] Maia F F Jr, Freire J A K, Farias G A, Freire V N and da Silva E F 2002 *J. Appl. Surf. Sci.* **190** 247
[22] Kassali K and Bouarissa N 2000 *Solid-State Electron.* **44** 501
[23] BenNasrallah S A, Sfina N and Said M 2005 *Eur. Phys. J.* B **47** 167
[24] Ben Zid F, Bhouri A, Mejri H, Tlili R, Said M, Lazzari J L, d'Avitaya F A and Derrien J 2002 *J. Appl. Phys.* **91** 9170
[25] Chen W Q and Andersson T G 1993 *J. Appl. Phys.* **73** 4484
[26] Sfina N, Lazzari J L, Ben Zid F, Bhouri A and Said M 2005 *Opt. Mater.* **27** 859
[27] Mejri H, Ben Zid F, Bhouri A, Ben Fredj A, Said M, Lazzari J L and Derrien J 2002 *Physica* B **322** 37
[28] Bhouri A, Mejri H, Ben Zid F, Belmabrouk H, Said M, Bouarissa N and Lazzari J L 2004 *J. Phys.: Condens. Matter* **16** 511